Mineralium Deposita (2001) 36: 165–176 

ARTICLE

Wouter Heijlen · Philippe Muchez · David A. Banks

# Origin and evolution of high-salinity, Zn–Pb mineralising fluids in the Variscides of Belgium

Received: 26 April 2000 / Accepted: 22 November 2000

**Abstract** High-salinity, Na–Ca–Cl-rich fluids (~20 wt% salts) in inclusions in gangue and ore minerals from Mesozoic Mississippi Valley-type (MVT) deposits in the Verviers Synclinorium (eastern Belgium) and in Cretaceous vein calcites at the Variscan front were investigated by microthermometric and crush-leach analysis. The MVT deposits formed at temperatures of ~110 °C while the Cretaceous vein calcites were precipitated at temperatures < 50 °C. Their Cl–Br content (Cl/Br ratio between 246 and 458) suggests that the fluids probably originated by the evaporation of seawater during basin development at the southern margin of the Caledonian Brabant Massif in the Late Palaeozoic. The Na–Ca–K content (Na: 29,700–49,600 ppm, Ca: 25,700–46,200 ppm, K: 1,000–5,620 ppm) is similar to that of the mineralising fluids in other Pb–Zn districts, interpreted to be of evaporative origin (e.g. Newfoundland, East Tennessee, Polaris). Furthermore, comparison of the Na–Ca–K content of the fluids with that of an evolved evaporitic brine enables the recognition of major water–rock interactions that modified the fluid composition. It indicates that the ambient fluids participated in the early diagenetic dolomitisation of Upper Palaeozoic carbonates and also in the albitisation of plagioclase in Lower Palaeozoic siliciclastics of the Caledonian basement. Illitisation of smectites or dissolution of K-feldspar probably controlled the K-content of the fluids. A model is proposed where the bittern brines migrated down into the deep subsurface because of their density during extension. After the Variscan orogeny, these fluids were finally expelled along extensional faults, resulting in the formation of Zn–Pb deposits.

Editorial handling: L. Diamond

W. Heijlen (✉) · P. Muchez
Fysico-chemische Geologie, K.U.Leuven,
Celestijnenlaan 200C, 3001 Heverlee, Belgium
e-mail: wouter.heijlen@geo.kuleuven.ac.be
Fax: +32-16-327981

D. A. Banks
School of Earth Sciences, University of Leeds,
Woodhouse Lane, Leeds LS2 9JT, UK

## Introduction

Post-Variscan migration of highly saline, Na–Ca–Cl fluids was widespread in central and western Europe (e.g. Behr et al. 1987, 1993; Wilkinson et al. 1995; Möller et al. 1997). These high-salinity fluids are present as fluid inclusions in minerals from Mississippi Valley-type (MVT) Pb–Zn deposits (Behr and Gerler 1987; Charef and Sheppard 1988; Redecke 1992). Movement of these fluids in the crust has been suggested to be fault-controlled (de Magnée 1967; Pelissonnier 1967; Behr et al. 1993). However, the origin of the fluids, how they gained their high salinity (~20 eq. wt% NaCl) and their composition remains unclear.

Based on fluid inclusion data and palaeogeographic considerations, Behr et al. (1987, 1993) proposed that the brines originated by the evaporation of seawater. Evaporation was widespread during the Permian and Mesozoic, causing the formation of thick anhydrite and halite deposits in central and western Europe. Although an evaporitic origin could clearly be invoked for the areas near or where these evaporites have been deposited, it can hardly explain the occurrence of post-Variscan high-salinity fluids in more confined areas without Mesozoic evaporites, such as in the Variscides of southern Belgium, or of Palaeozoic high-salinity fluids in western Europe (Dejonghe et al. 1982; Samson and Russell 1987; Banks and Russell 1992). At the Variscan front zone in Belgium, high-salinity fluids were expelled during several periods in the Mesozoic (Muchez et al. 1997; Muchez and Sintubin 1998) and formed the MVT Zn–Pb deposits in the Verviers Synclinorium, eastern Belgium (Darimont 1983; Fig. 1). First microthermometric data on these Zn–Pb deposits indicate constant salinities of ~20 eq. wt% NaCl (Darimont 1983; Redecke 1992) and a decrease in the formation temperature of the successive calcite generations from ~125 to ≤50 °C (Muchez et al. 1994).

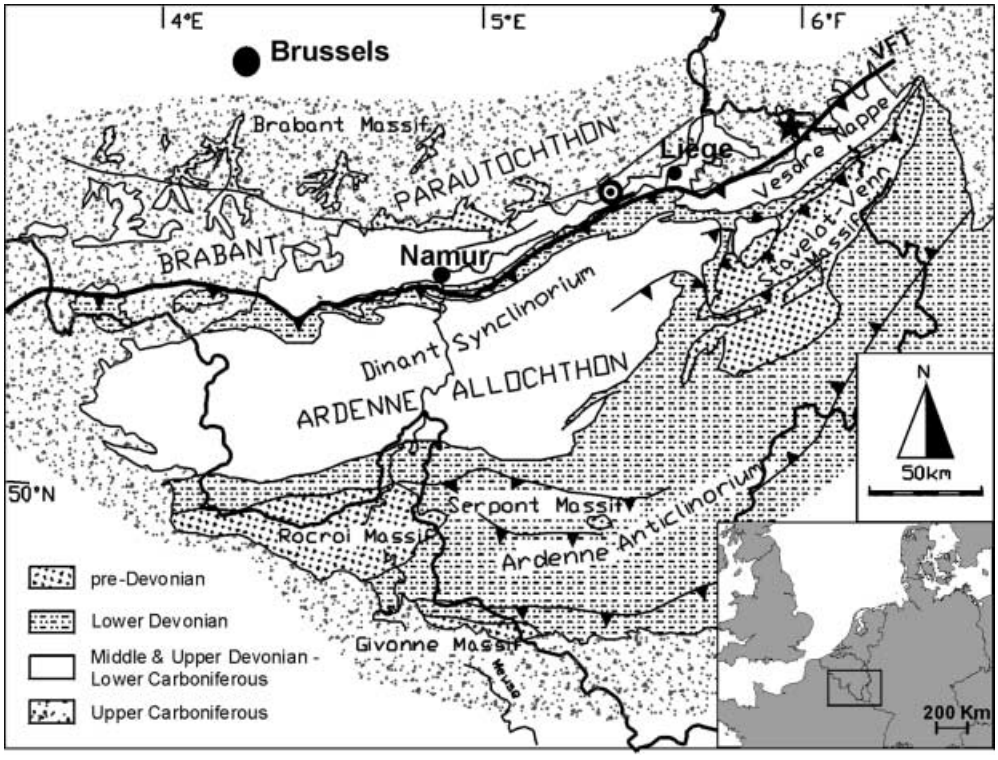


**Fig. 1** Location of the samples studied in Belgium. *VFT* Variscan Front Thrust. *Circle* post-Variscan, non-mineralised calcite veins; *star* Bleiberg Zn–Pb mineralisation

Structural relationships suggest that the mineralisation in the area occurred in one main period between the Upper Carboniferous and the Upper Cretaceous (de Magnée 1967; Dejonghe 1986; Muchez et al. 1997). Rb–Sr dating of sphalerites from the Maubach and Mechernich Pb–Zn deposits in the nearby Eifel gives an age of 170 ± 4 Ma (Schneider et al. 1999).

From the Jurassic onwards, the Verviers Synclinorium was bordered by the antiformal structures of the Caledonian Brabant Massif in the NW and the Variscan Ardennes in the SE and it has been subjected to a continuous peneplanation until the Cretaceous. The only Mesozoic strata at the Variscan front zone are Upper Cretaceous marls and chalks, which are younger than the mineralisation. However, there are abundant evaporites in the Devonian and Carboniferous of southern Belgium (Groessens et al. 1979; Rouchy et al. 1986; Dejonghe and Boulvain 1993; De Putter et al. 1994). Givetian anhydrites reach a total thickness of 300 m (Rouchy et al. 1986), and 760 m of Dinantian evaporites occur in the St-Ghislain borehole (Groessens et al. 1979). High-salinity fluids generated during Devono-Carboniferous evaporation could well be the source of the mineralising fluids. In this scenario, the mineralising fluids remained in the subsurface since their formation during the Devono-Carboniferous until they were expelled in the Mesozoic. However, Cauet and Weis (1983) and Dejonghe (1985) suggested that these residual brines had already been expelled during the Variscan orogeny. Therefore, they concluded that deeply circulating post-Variscan meteoric waters that dissolved evaporites in the subsurface were responsible for the mineralisation. This model was further supported by a stable isotope analyses of gangue calcites (Muchez et al. 1994).

The purpose of this study is to investigate the origin of the high-salinity, mineralising fluids present at the Variscan front zone and to deduce the geochemical evolution of these fluids in the deeper subsurface. To differentiate between an evaporative or evaporite-dissolution origin of the high-salinity fluids, Cl–Br systematics can be used (Carpenter 1978; Fontes and Matray 1993). The further interaction of the fluid with the rocks can be deduced from its cation composition.

## Geological setting

The Zn–Pb deposits of eastern Belgium are present in Devonian and Carboniferous strata. The Devono-Carboniferous series have been deposited above a folded and faulted Caledonian basement, composed mainly of quartzites, shales and siltstones. Early Devonian siliciclastic rocks lie unconformably on this basement. They are overlain by alternating siliciclastics and carbonate rocks, which are interlayered with evaporites of Middle and Late Devonian and Dinantian age. All the Palaeozoic rocks have been affected by the Variscan orogeny. The Variscan Front Thrust, also referred to as the Midi-Aachen fault zone, separates the Ardenne Allochthon in the south from the Brabant Parautochthon in the north (Fig. 1). This fault zone is fringed at its footwall by numerous smaller thrust sheets and imbricate fans (Hance et al. 1999).

The total production of the zinc-lead district in eastern Belgium is some 1.1 Mt of zinc and 0.13 Mt of lead metal (Dejonghe and Jans 1983). Mine activity in the area ceased in 1946. Although small in comparison with present day world class deposits, the area played a very important role in the metal industry from the Middle Ages to the 19th century. The first industrial process for the manufacturing of metallic zinc was developed here by J.J. Daniel Dony in the beginning of the 19th century (Ladeuze et al. 1991).

Around 30 mines were active in the area, the larger ones being La Calamine, Schmalgraff and Bleiberg. The main gangue minerals are calcite and quartz. Ore mineralogy and morphology of the different deposits in the district are described in detail by Dejonghe and Jans (1983) and Dejonghe (1986, 1998). A regional Pb isotopic study indicated that the metals were mainly leached from the Middle and Upper Devonian sedimentary units (Cauet et al. 1982; Cauet and Weis 1983). The formation of the Zn–Pb deposits and of post-Variscan calcite veins has been related to Mesozoic extensional and transpressive tectonism (de Magnée 1967; Muchez and Sintubin 1997; Muchez et al. 1997). The Zn–Pb mineralisations are spatially controlled by NNW-trending transverse faults that are related to the Rhine graben fault system (de Magnée 1967; Dejonghe and Jans 1983).

In this study, we have investigated calcite, quartz and sphalerite associated with the Bleiberg deposit in eastern Belgium (Dejonghe and Jans 1983) and calcite cements in a non-mineralised, dextral strike-slip fault system in the Variscan Front Complex (Muchez and Sintubin 1998). Bleiberg is one of the most important, fault-controlled deposits in the Dinantian carbonate rocks and Namurian shales. This 2-km-long vein deposit, which strikes NNW, repeatedly crosscuts these deformed strata and is accompanied by some lodes at lithological and tectonic contacts. The samples have been taken from the drillings of the exploration company Nicron France S.A., which crosscut a newly discovered extension of the Bleiberg deposit. The calcite cements filling the dextral strike-slip fault have been selected as they are characterised by similar high-salinity fluids as those associated with the Zn–Pb ore deposits (Muchez and Sintubin 1998).

## Methodology

Thin sections of the vein cements were examined by conventional and cathodoluminescence (Cl) microscopy. The Technosyn Cold Cathodo Luminescence Model 8200 MkII was operated at 16–20 kV, 620 μA gun current, 5 mm beam width and 6.65 Pa vacuum. Microthermometric analysis of fluid inclusions in gangue minerals was carried out on a Fluid Inc. adapted USGS gas-flow heating/freezing stage. The fluid inclusions in the nearly opaque sphalerites were studied using a Linkam THMSG 600 stage together with an Olympus BX-60 microscope modified for IR illumination. Only one- and two-phase aqueous fluid inclusions were identified. The temperatures of first melting (Tfm) and the melting of ice [Tm(ice)] were carefully measured. Reproducibility was within 0.2 °C. The stages were calibrated between −56.6 and 374.1 °C with synthetic fluid inclusions. Melting temperatures in one-phase fluid inclusions in calcite and quartz were obtained after artificial stretching by heating the inclusions to 200 °C followed by freezing at −100 °C in order to initiate a gas bubble. Only few temperature measurements of hydrohalite melting could be made and these gave inconsistent results. These data have not been incorporated. Salinities were reported as eq. wt% NaCl (Bodnar 1993) or eq. wt% $CaCl_2$ if Tm(ice) was $< -21.2$ °C (Oakes et al. 1990). This results in errors of $< 3$ wt% on the total wt% NaCl + $CaCl_2$.

Analysis of fluid inclusions was carried out using a bulk crush-leach method as described by Bottrell et al. (1988), Banks and Yardley (1992) and Yardley et al. (1993). Samples were crushed to a grain size of ∼1 mm and cleaned in aqua-regia where appropriate. Contaminated mineral grains were removed by hand picking under a binocular microscope and the samples further cleaned by boiling in nitric acid and/or doubly-distilled water. Quartz samples had any absorbed ions removed by placing them in an electrolytic cell for 10 days. Clean, dry samples were crushed to a fine powder in an agate pestle and mortar and leached in doubly-distilled water for anion and alkali analysis, and in acidified $LaCl_3$ solution for other cation analysis on the quartz samples. Carbonates and quartz were analysed for Na, K and Li by flame emission spectroscopy (FES). Cl and Br were analysed by ion chromatography. Acid leaches from quartz were analysed for other cations by inductively coupled plasma atomic emission spectroscopy (ICP-AES). Na and K were determined on all leach solutions from all minerals, so that all analyses were calculated initially as ratios to Na. For the calcites, Ca was calculated to give a charge balance with the anions. The analyses were rearranged to be ratios to Cl and absolute concentrations were calculated using the salinity of the primary fluid inclusions obtained from the microthermometric analyses. Because of the small volumes of solution available from the quartz samples, anions could not be measured. The quantification of the Na, K, Mg and Ca concentration in the fluid inclusions in the quartz samples was carried out according to the method of Weisbrod and Poty (1975) and Shepherd et al. (1985). According to these authors, the contribution of $CaCl_2$ and $MgCl_2$ to the freezing point depression is 1.5 times that of NaCl and KCl. For these samples the Cl concentration was calculated to give charge balance with the cations.

## Petrography and fluid inclusion microthermometry

### Zn–Pb mineralisation at Bleiberg

The paragenetic sequence of the ore and gangue minerals of the Bleiberg deposit was reconstructed based on crosscutting relationships (Fig. 2). After the precipitation of two generations of ferroan calcite (stages A and B), the main sulphide minerals (sphalerite, galena) formed. Ore mineralisation started with sphalerite replacing carbonates, as represented by rounded subhedral grains of sphalerite with relict carbonate in the porous centre (Fig. 3a). The replacive sphalerite is often cemented and overgrown by quartz. The remaining open spaces were filled by blocky sphalerite and galena (Fig. 3b), which sometimes have inclusions of chalcopyrite, pyrite and marcasite. This period of ore mineralisation was followed by the precipitation of second generation quartz around the sulphides. The quartz is succeeded by three generations of ferroan calcite (stages C, D and E; Fig. 2). All calcite generations show a bright yellow luminescence, except for the dull brown-orange luminescent stage A calcite.

Primary fluid inclusions could be identified in growth zones in second generation quartz , sphalerite and calcite. The Tfm of these inclusions is ∼−52 °C, indicative of an $H_2O$–NaCl–$CaCl_2$ fluid (Shepherd et al. 1985). The primary inclusions in quartz (Fig. 3c) are mono- and two-phase and can be up to 50 μm large. The Th of the two-phase fluid inclusions is mostly between 97 and 115 °C (Fig. 4a). Occasionally, homogenisation temperatures above 115 °C were measured ($n = 3$ in Fig. 4a). These higher temperatures are caused by necking down and were not taken into account. Tm(ice) varies between −14.0 and −17.2 °C (Fig. 4c). In sphalerite, all primary inclusions (5–20 μm) are two-phase with Th between 97 and 108 °C and Tm(ice) between −15.9 and −16.9 °C (Figs. 3d and 4a, d). The primary inclusions in the different calcite generations have previously been studied by Muchez et al. (1994). The Th values are ∼120 °C in calcite generations A and B and decrease to values between 97 and 68 °C in calcite generation C (Fig. 4b). The last two calcite generations only contain one-phase inclusions in which no bubble appeared after several cooling

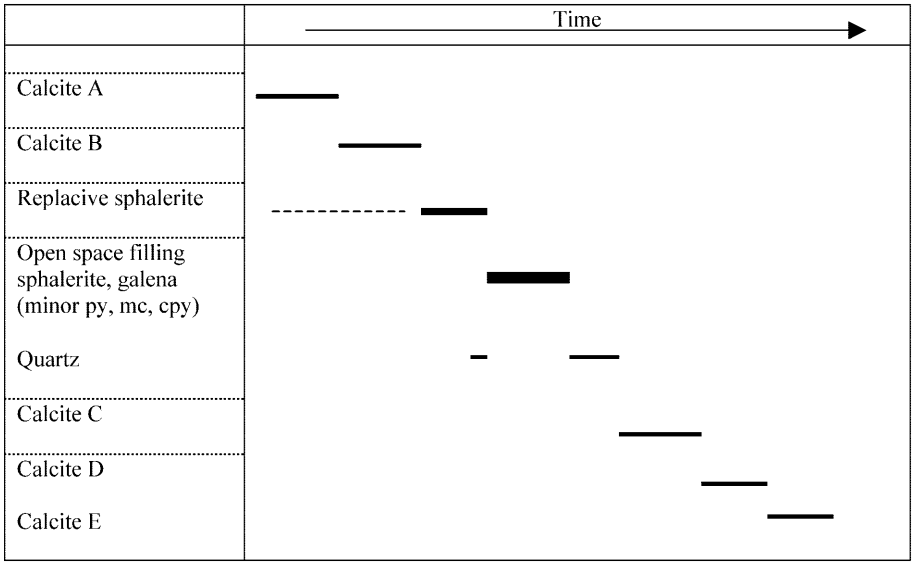


**Fig. 2** Generalised paragenetic sequence of the Zn–Pb mineralisation at Bleiberg. *py* Pyrite; *mc* marcasite; *cpy* chalcopyrite

attempts. Most Tm(ice) values in all calcite generations vary between −12.0 and −21.1 °C (Figs. 3e and 4e, f).

In all investigated samples, pseudosecondary and secondary inclusions are present. The pseudosecondary inclusions are small, rounded and one- or two-phase (1–5 μm). The Tfm, Th and Tm(ice) values are similar to those of the primary inclusions in the different minerals (Fig. 4c, d). These inclusions are abundant in the quartz and sphalerite samples, but scarce in calcite. The secondary inclusions are often large (20–100 μm), irregular and almost always one-phase. Their Tm(ice) is between −0.5 and −4.5 °C and the Tfm of ∼−20 °C indicates that they only contain an $H_2O$–NaCl fluid (Fig. 3e, f). Secondary fluid inclusions are scarce in the quartz and sphalerite samples, but quite common in the calcite.

Calculated salinities for the primary and pseudosecondary inclusions range between 17.8 and 20.4 eq. wt% NaCl in the quartz samples, from 18.1 to 20.2 eq. wt% NaCl in the sphalerites and from 16.0 to 23.1 eq. wt% NaCl in the calcites. The secondary inclusions in the calcites have a salinity between 0.9 and 7.2 eq. wt% NaCl.

## Post-Variscan non-mineralised calcite cements

A non-ferroan followed by a ferroan calcite generation has been recognised in vein samples along a dextral strike-slip fault system at the Variscan Front Complex (Muchez and Sintubin 1998). The non-ferroan (calcite a) and ferroan calcites (calcite b) show a dark brown to brown-orange and a bright brown-orange luminescence, respectively. One- and two-phase fluid inclusions are present in growth zones and are between 4 and 60 μm large. The Th values of the primary, two-phase inclusions in both the non-ferroan and ferroan calcites are between 37 and 65 °C. The first melting temperature of all primary fluid inclusions is ∼ −52 °C, indicating an $H_2O$–NaCl–$CaCl_2$ composition. Tm(ice) values are between −14.8 and −28.8 °C (Fig. 5a, b). Secondary inclusions are abundant and contain two fluid types. The Th of all secondary inclusions varies from ≤50 to 131 °C (Muchez and Sintubin 1998). The first fluid type is characterised by a Tfm of around −52 °C and Tm(ice) ranges between −11.2 and −28.6 °C. The second, less abundant fluid type, has a Tfm of ∼ −21 °C and Tm (ice) values between 0.0 and −4.6 °C. The salinities for the primary and secondary inclusions of the $H_2O$–NaCl–$CaCl_2$ system are between 17.1 and 24.4 eq. wt% $CaCl_2$. The secondary $H_2O$–NaCl fluid inclusions have a salinity between 0.0 and 7.3 wt% NaCl.

## Fluid inclusion geochemistry

Fluid inclusions from calcite and quartz samples from the Bleiberg deposit and samples from the non-mineralised calcite veins, containing similar high-salinity fluids, have been analysed for their ionic composition. The molar ratios of the analysed elements against Na are reported in Table 1 while the reconstructed fluid composition is shown in Table 2. Fluid inclusion petrography and microthermometry indicate the presence of secondary, low-salinity fluid inclusions. Because this second fluid is characterised by a low salinity and because the geochemical composition of the mineralising fluids has been calculated based on the salinity of the primary inclusions, this second fluid has no influence on the calculated chemistry of the mineralising fluids.

The molar Cl/Br and Na/Br ratios of all fluids analysed (Fig. 6) are very similar to those reported for Zn–Pb mineralising fluids from East Tennessee, Newfoundland, Pine Point, Polaris and Cracow–Silesia (group I, Fig. 6), which all have Cl/Br and Na/Br ratios significantly lower than those of seawater (Kesler et al.

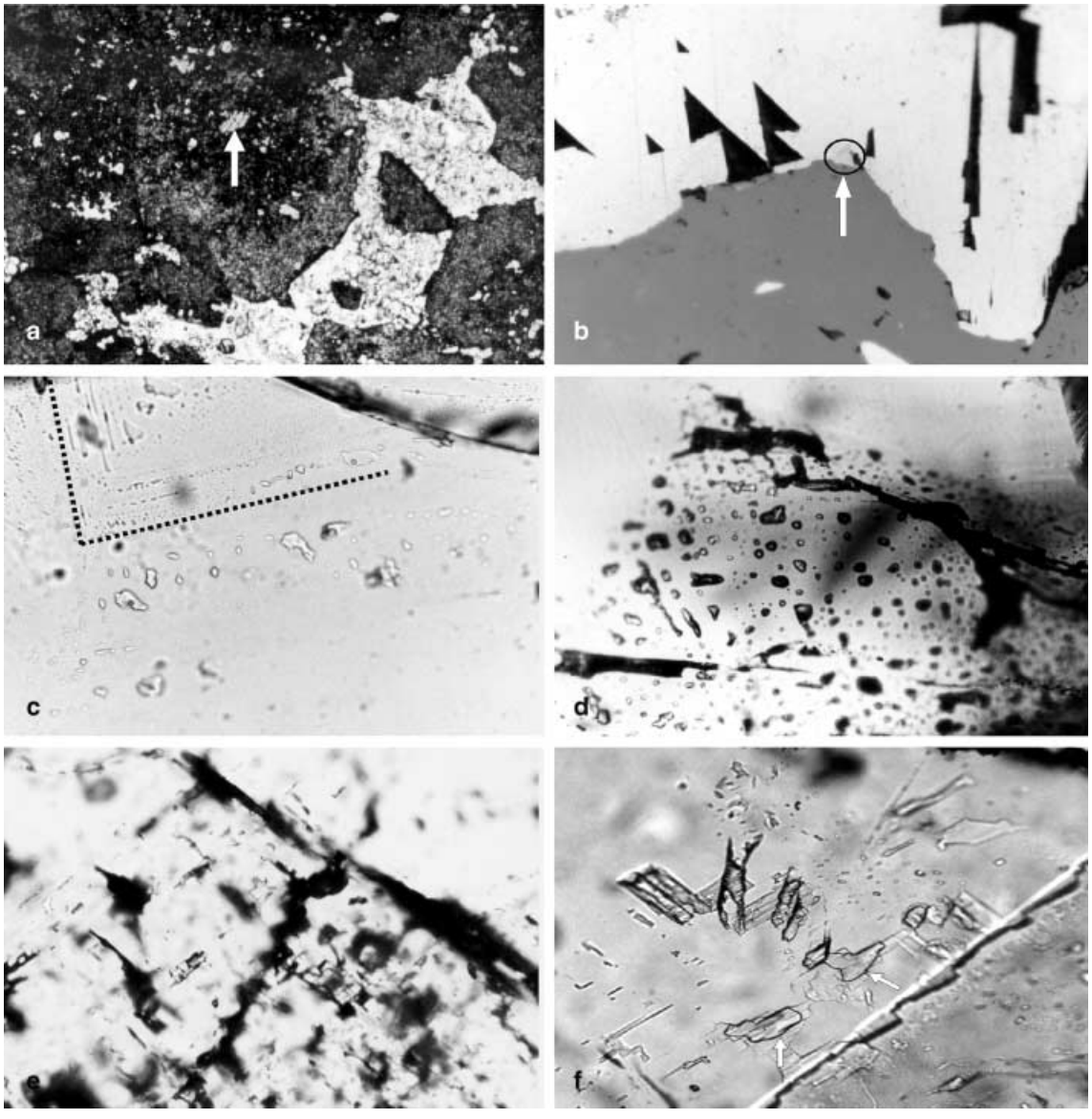


**Fig. 3** Photomicrographs of the ore and gangue minerals and their fluid inclusions in the Bleiberg deposit. **a** Subhedral, replacive sphalerite grains, cemented by blocky quartz (*white*). Twinned carbonate remnant in the centre of a sphalerite grain (*arrow*). Length of photograph is 1 mm. Plane-polarised transmitted light. **b** Massive sphalerite and galena with inclusions of chalcopyrite (*arrow*). Length of photograph is 0.2 mm. Plane-polarised reflected light. **c** One- and two-phase fluid inclusions in a growth zone (indicated by the *hatched line*) in late-stage quartz. Length of photograph is 0.5 mm. **d** Two-phase fluid inclusions in a growth zone in sphalerite. Length of photograph is 0.5 mm. **e** Two-phase, primary fluid inclusions in a growth zone in stage C calcite. Length of photograph is 1 mm. **f** Large (>100 μm), secondary fluid inclusions in stage C calcite, showing a large volume percentage occupied by the irregular vapour phase (*arrows*) caused by artificial stretching. Length of photograph is 1 mm

1996; Viets et al. 1996). Mineralising fluids from the North Arkansas, Tri-State, Viburnum Trend, central Missouri, southern Illinois, Upper Mississippi Valley and central Tennessee districts (group II, Fig. 6) have Cl/Br and Na/Br ratios between those of the first group and seawater (e.g. early stage fluids in Viburnum trend; Crocetti and Holland 1989) or even higher (Viets and Leach 1990; Kesler et al. 1995, 1996; Viets et al. 1996). The K/Na ratios of the fluids analysed (0.0122 to 0.1078) fall in the range of typical Mississippi Valley-type fluids, which have K/Na ratios that are distinctively higher than those of modern oil-field brines (Leach and Sangster 1993).

Using the calculated fluid composition, all analyses plot at or below the Seawater Evaporation Trajectory (SET; Carpenter 1978; Connolly et al. 1990) on a log Cl–log Br diagram (Fig. 7a) and beyond the point of halite precipitation. Salinities below this point suggest mixing of the brine with a dilute fluid. For example, mixing of a brine that was evaporated to a degree of 15 to 25 times the seawater concentration with maximal 20% of a low-salinity fluid (meteoric or seawater) could account for the Cl–Br data. This cannot be the result of

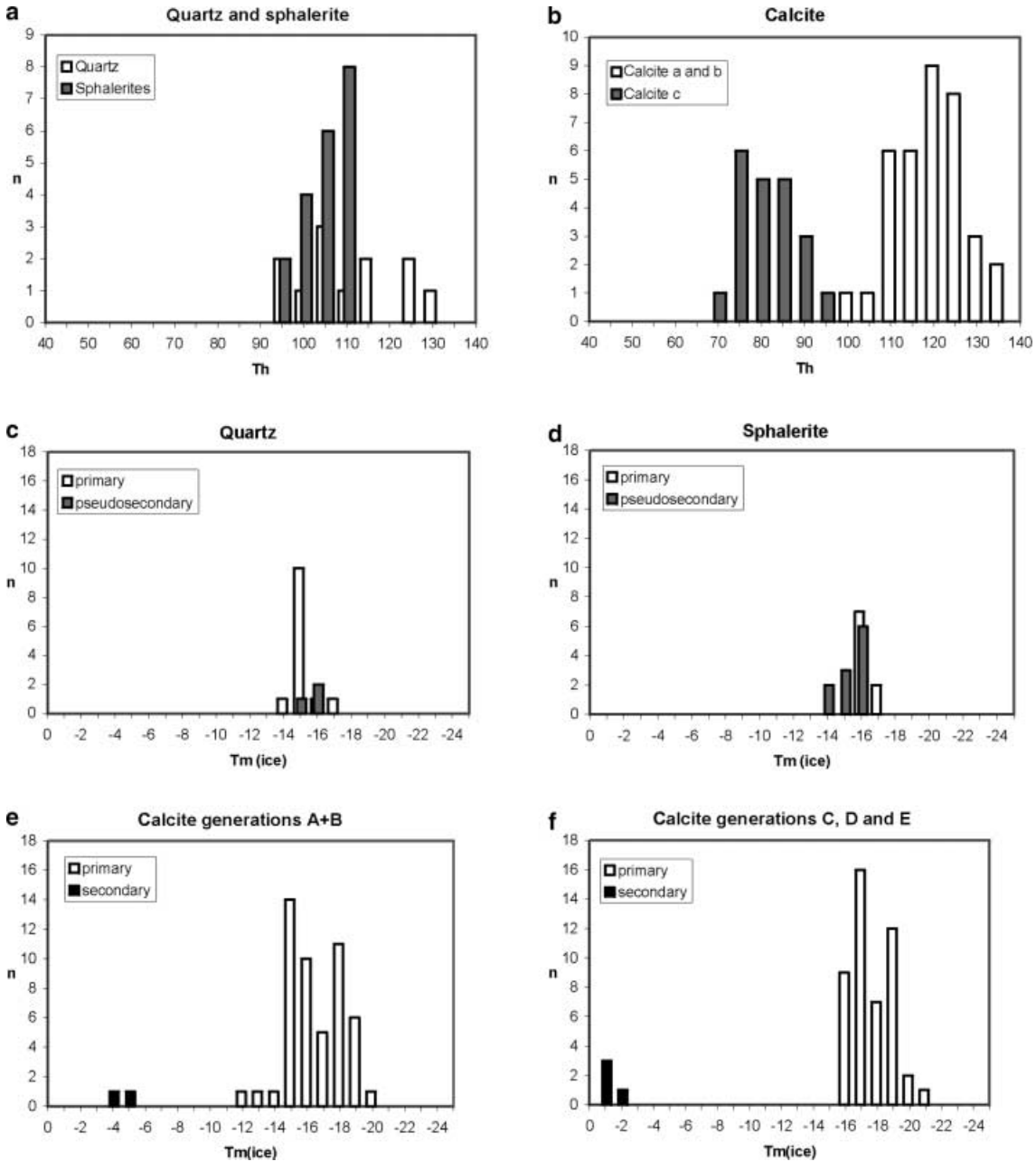


**Fig. 4a–f** Homogenisation and ice melting temperatures of primary, pseudosecondary and secondary fluid inclusions in minerals associated with the Zn–Pb deposit Bleiberg. Calcite data partly after Muchez et al. (1994)

mixing with low-salinity, secondary fluid inclusions during the analyses because quantification of the Cl and Br content was made using the salinity of the primary inclusions in the calcites.

The Li/Na ratio of the fluids is between 0.00331 and 0.00596 which is much higher than that expected if the fluids originated by dissolution of evaporites (Li/Na ratios between 0.00030 and 0.00200; Bodine and Jones 1990). The mineralised and non-mineralised veins cannot be distinguished on the basis of the Cl–Br data or Li/Na ratios. In comparison with evaporated seawater, all fluids analysed show a deficit in Na and an excess in Ca (Fig. 7b, c). Davisson and Criss (1996) showed that a plot of '$Ca_{excess}$' versus '$Na_{deficit}$'(expressed in milliequivalents per liter) can help in recognising processes that affect the evolution of basinal fluids. The co-ordinates are given by the mathematical expressions:

$$Ca_{excess} = \{Ca_{meas} - (Ca/Cl)_{sw}\ Cl_{meas}\}2/40.08$$

and

$$Na_{deficit} = \{(Na/Cl)_{sw}\ Cl_{meas} - Na_{meas}\}1/22.99$$

where *sw* and *meas* refer, respectively, to seawater and measured concentrations (in mg/l). The numerical constants convert the result to milliequivalent/l. In this

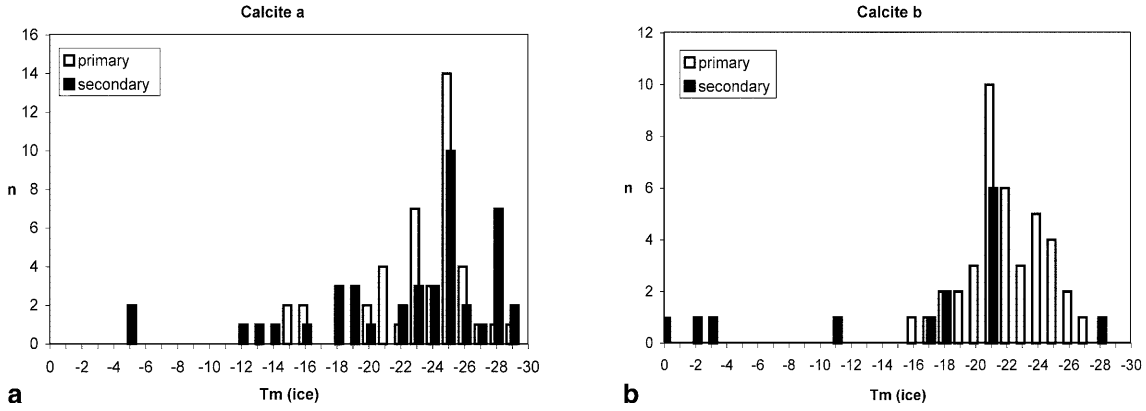


**Fig. 5** Ice melting temperatures of primary fluid inclusions in **a** non-ferroan and **b** ferroan calcites occurring along a strike-slip fault (Variscan Front Complex). Data partly after Muchez and Sintubin (1998)

plot, processes such as evaporation of seawater and halite dissolution, as well as water-rock interactions that affect the Ca and/or Na content of the fluids show distinct trends. Because the crush-leach data are expressed in milligram per kilogram solution, we used

**Table 1** Molar ratios of fluid inclusion leachates from calcites (*C*) and quartz (*Q*) associated with zinc–lead mineralisation (*) and barren vein calcites ($\sigma$ = ~10%)

| Sample | Ca/Na | K/Na | Mg/Na | Li/Na | Cl/Na | Br/Na | Cl/Br |
|---|---|---|---|---|---|---|---|
| NB183 (C*) | – | 0.0176 | – | 0.00484 | 1.75 | 0.00585 | 299 |
| NB192 (C*) | – | 0.0188 | – | 0.00398 | 1.69 | 0.00515 | 328 |
| NB178 (C*) | – | 0.0188 | – | 0.00404 | 1.68 | 0.00500 | 336 |
| NB156 (C*) | – | 0.0181 | – | 0.00512 | 1.70 | 0.00613 | 277 |
| NB177 (C*) | – | 0.0122 | – | 0.00231 | 1.69 | 0.00369 | 458 |
| FO30A (C) | – | 0.0481 | – | 0.00364 | 2.57 | 0.00955 | 269 |
| FO31A (C) | – | 0.0432 | – | 0.00431 | 2.08 | 0.00847 | 246 |
| FO36A (C) | – | 0.0542 | – | 0.00331 | 2.09 | 0.00836 | 250 |
| FO30B (C) | – | 0.0437 | – | 0.00331 | 1.97 | 0.00799 | 247 |
| FO38B (C) | – | 0.0584 | – | 0.00596 | 1.88 | 0.00561 | 335 |
| NB289 (Q*) | 0.397 | 0.0821 | 0.0024 | – | – | – | – |
| NB214 (Q*) | 0.444 | 0.0717 | 0.0210 | – | – | – | – |
| NB218 (Q*) | 0.548 | 0.1078 | 0.0302 | – | – | – | – |
| NB253 (Q*) | 0.509 | 0.0842 | 0.0319 | – | – | – | – |
| NB257 (Q*) | 0.579 | 0.0532 | 0.0291 | – | – | – | – |

**Table 2** Reconstructed fluid composition of the leachates from calcites (*C*) and quartz (*Q*) associated with zinc-lead mineralisation (*) and barren vein calcites

| Sample | Salinity[a] *($\sigma$ ; n)* | Reconstructed fluid composition (ppm) | | | | | | |
|---|---|---|---|---|---|---|---|---|
| | | Na | Ca[b] | K | Mg | Li | Cl[c] | Br |
| NB183 (C*) | 19.5 *(5 ; 22)* | 43,800 | 28,700 | 1,310 | – | 64 | 118,000 | 890 |
| NB192 (C*) | id. | 45,500 | 29,200 | 1,450 | – | 55 | 118,000 | 810 |
| NB178 (C*) | 20.3 *(4 ; 23)* | 47,500 | 30,800 | 1,520 | – | 58 | 123,000 | 830 |
| NB156 (C*) | 21.5 *(3 ; 16)* | 49,600 | 31,500 | 1,530 | – | 77 | 130,000 | 1,060 |
| NB177 (C*) | 20.6 *(4 ; 18)* | 48,000 | 32,300 | 1,000 | – | 33 | 125,000 | 620 |
| FO30a (C) | 21.2 *(11 ; 36)* | 34,200 | 46,200 | 2,800 | – | 38 | 135,000 | 1,140 |
| FO31a (C) | 23.0 *(4 ; 28)* | 45,800 | 42,600 | 3,360 | – | 60 | 147,000 | 1,350 |
| FO36a (C) | 21.4 *(10 ; 21)* | 42,500 | 39,300 | 3,910 | – | 42 | 137,000 | 1,240 |
| FO30b (C) | 21.7 *(5 ; 21)* | 45,800 | 38,000 | 3,400 | – | 46 | 139,000 | 1,270 |
| FO38b (C) | 20.7 *(8 ; 27)* | 45,600 | 35,700 | 4,530 | – | 82 | 132,000 | 890 |
| NB289 (Q*) | 18.7 *(3 ; 13)* | 37,100 | 25,700 | 5,180 | 95 | – | 108,000 | – |
| NB214 (Q*) | id. | 34,600 | 26,800 | 4,220 | 769 | – | 107,000 | – |
| NB218 (Q*) | id. | 30,700 | 29,300 | 5,620 | 977 | – | 107,000 | – |
| NB253 (Q*) | id. | 31,900 | 28,300 | 4,570 | 1,076 | – | 107,000 | – |
| NB257 (Q*) | id. | 29,700 | 30,000 | 2,690 | 914 | – | 104,000 | – |

[a] Salinity for calcites (*C*) and quartz (*Q*) associated with mineralisation (*) in eq. wt% NaCl; for calcites in non-mineralised veins in eq. wt% $CaCl_2$. $\sigma$ = standard deviation (%), *n* = number of measurements

[b] Ca concentration for calcites based on charge balance

[c] Cl concentration for quartz based on charge balance

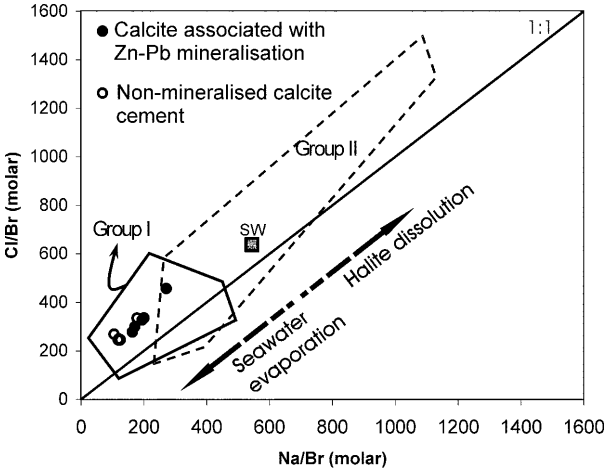


**Fig. 6** Na–Cl–Br compositions of the samples analysed compared with other Mississippi Valley-type fluids. The *filled square* refers to the seawater value (SW). *Filled dots* Calcite associated with Zn–Pb mineralisation; *open dots* non-mineralised calcite cements. *Group I* East Tennessee, Newfoundland, Pine Point, Polaris and Cracow Silesian districts; *Group II* North Arkansas, Tri-State, Viburnum Trend, central Missouri, southern Illinois, Upper Mississippi Valley and central Tennessee districts. Group I and II data after Crocetti and Holland (1989), Viets and Leach (1990), Kesler et al. (1995, 1996), Viets et al. (1996)

these units in the reconstruction of the excess-deficit plots. When $CaSO_4$ and $CaCO_3$ attain saturation during evaporation of seawater, the fluid will follow a vertical descent from the origin until virtually all Ca is lost (Fig. 8a). From halite saturation onwards, the fluid composition is shifted towards a greater $Na_{deficit}$. For fluids that originated by the evaporation of seawater, deviations from this horizontal SET are the result of water-rock interactions or mixing between fluids. All fluids analysed plot well above the SET in the field of $Ca_{excess}$ and show a linear trend. Despite the microthermometric evidence for a Ca–Na–Cl dominated fluid, it should be noticed that the Ca content of the fluids in the calcites was calculated to give charge-balance with the anions. Therefore, the presence of other cations (especially $Mg^{2+}$) could result in an overestimation of the excess Ca for the fluids in the calcites. However, the analyses of the fluid inclusions in the quartz samples, where $Mg^{2+}$ was measured as well, confirm the high Ca and very low Mg content of the mineralising fluids (Table 2). The simultaneous increase in $Ca_{excess}$ and $Na_{deficit}$ compared with that predicted for seawater that was evaporated to the observed degree (Fig. 8a), suggests a 1 Ca to 2 Na exchange reaction. However, the observed $Ca_{excess}$ is too high to be explained solely by such a reaction. The processes by which an additional

**Fig. 7** Log–log plots of major cations Na, Ca, K and of Br in the fluids versus Cl. The *dashed lines* in **a** represent the percentage of mixing with meteoric water (20, 40, 60 and 80%). *SET* Seawater Evaporation Trajectory (data from McCaffrey et al. 1987)

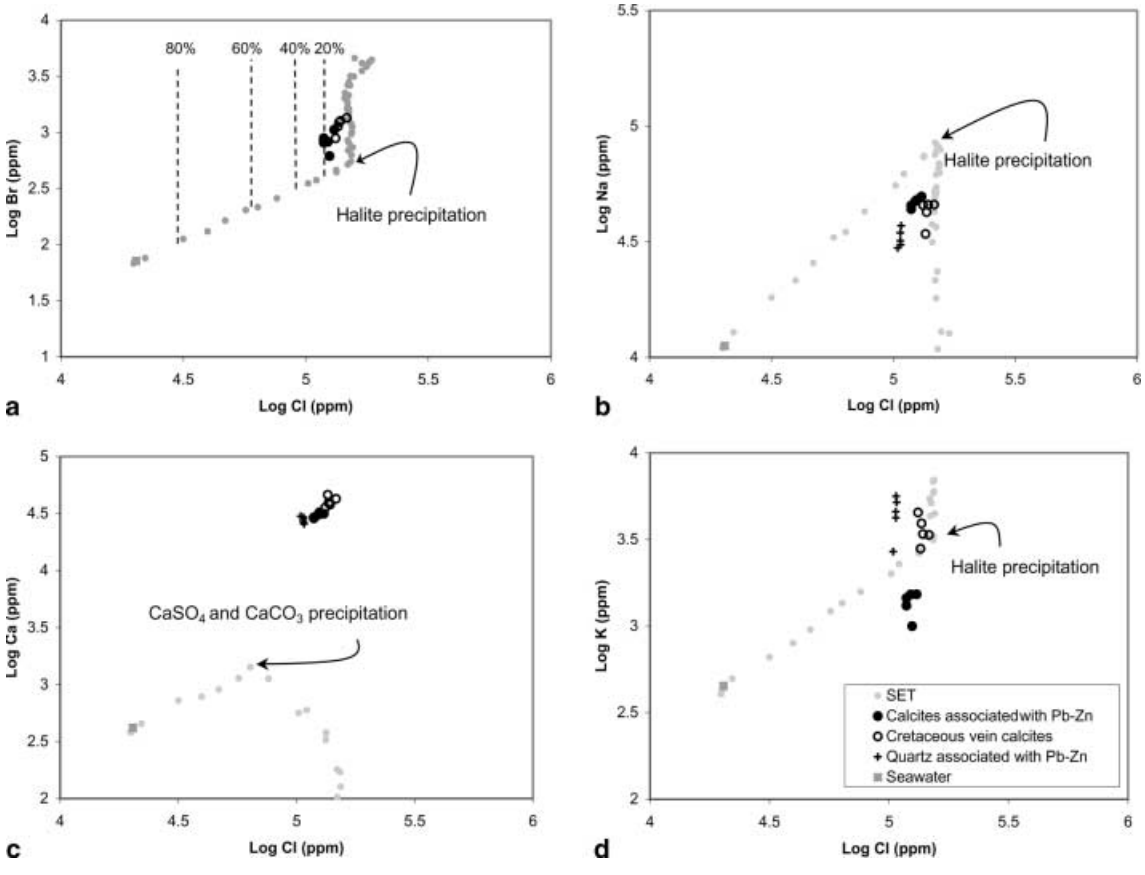

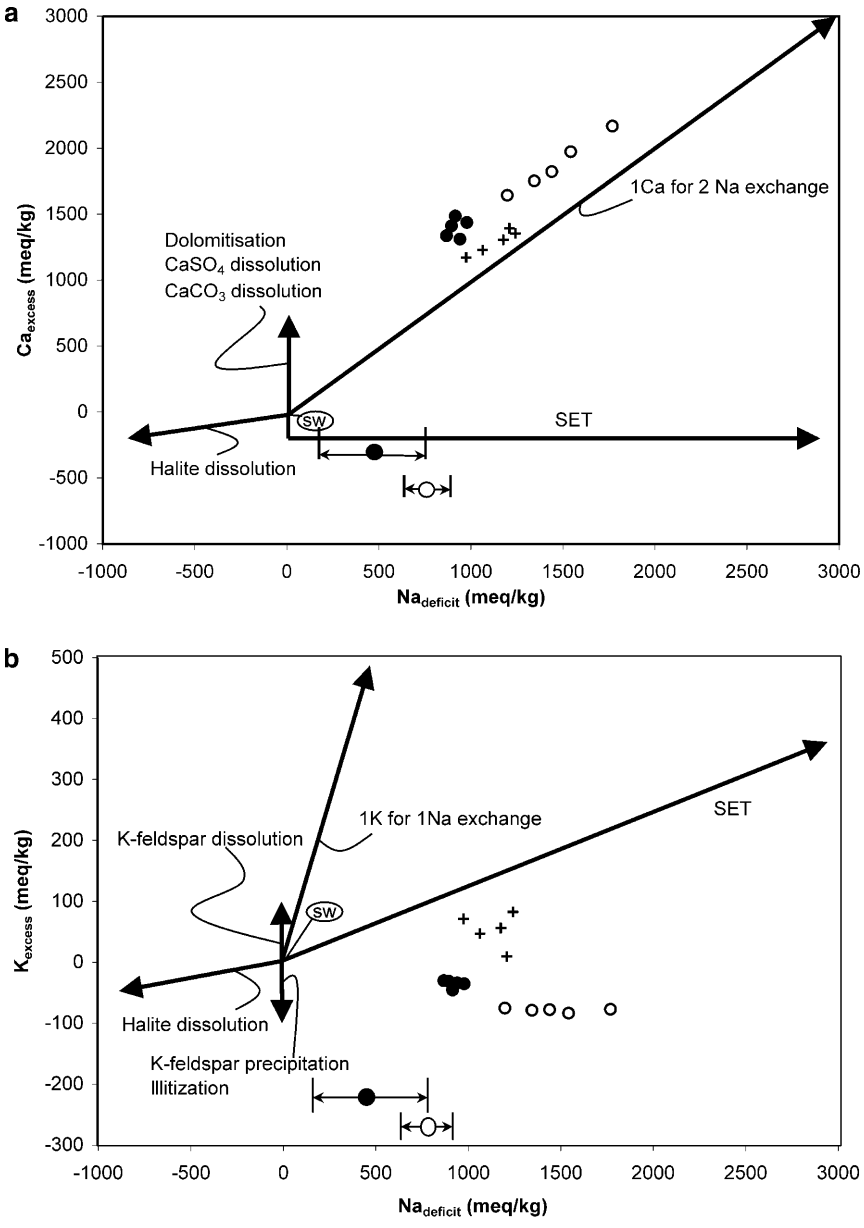


**Fig. 8** **a** $Ca_{excess}$–$Na_{deficit}$ plot of fluid inclusions in post-Variscan calcites and quartz (after Davisson and Criss 1996). The *bold lines* represent the predicted trajectories for the different indicated processes. Note that when using milliequivalent per kg solution units, an exchange of $2Na^{+}$ for $1Ca^{2+}$ produces a 1:1 trend. Also indicated are the ranges of the expected $Na_{deficit}$ for seawater that is evaporated to the observed degree for the different fluids analysed. **b** $K_{excess}$–$Na_{deficit}$ plot. *Symbols* as in Fig. 7

increase in the Ca content can take place without changing the Na content are dolomitisation and $CaSO_4$ or $CaCO_3$ dissolution. Microthermometric data indicates that Ca is mainly balanced by chloride which makes dolomitisation the most likely process to dominate this increase. In addition, the sulphate content measured in some crush-leach analyses of calcites was below 6,800 ppm ($SO_4^{2-}$/Na between 0.02 and 0.14). Because of the low solubility of $CaCO_3$, carbonate species cannot be responsible for the charge balance of these high-salinity fluids.

Similarly, the '$K_{excess}$' of a brine can be defined as:

$$K_{excess} = \{K_{meas} - (K/Cl)_{sw}\, Cl_{meas}\}1/39.1$$

An evaluation of the enrichment or depletion in K is not straightforward from a log Cl–log K plot (Fig. 7d), because of the variable degree of evaporation of the fluids. A plot of the $K_{excess}$ versus the $Na_{deficit}$ (Fig. 8b) clearly visualises the depletion in K of the different analysed fluids compared with evolved seawater. The $K_{excess}$ is not linearly correlated with the $Na_{deficit}$. Precipitation and dissolution of K-feldspar and illitisation probably influence the potassium content of basinal brines (e.g. Carpenter et al. 1976; Land and Prezbindowski 1981). These processes do not or only very slightly change the Na content of the brines. It is probable, therefore, that they account for the deviations from the SET line in the $K_{excess}$–$Na_{deficit}$ plot.

## Discussion

The decrease in homogenisation temperature of the fluid inclusions in the successive stages of the paragenetic

sequence of the mineralisation (Figs. 2 and 4a, b), was already noted by Muchez et al. (1994). They argue that the homogenisation temperatures have to be pressure-corrected by less than 8 °C. Salinities remain fairly constant throughout the different paragenetic stages, although the fluid inclusions in the quartz and sphalerite samples have salinities at the lower end of the salinity range. So, the decrease in temperature is not associated with a change in the salinity. This seems to exclude a decrease in temperature caused by mixing with low-temperature, surficial, low-salinity fluids. The decrease could, for example, be caused by a slower upward migration of the fluids, allowing an increase in the thermal equilibrium with the surrounding rocks. However, other possibilities, such as a shallower origin in the basement for the mineralising fluids, cannot be ruled out. Both the temperature of formation and salinities are similar to those reported from deposits in other MVT districts (Anderson and Macqueen 1982; Leach and Sangster 1993).

The Frasnian and Dinantian limestones were dolomitised early during diagenesis (Dejonghe et al. 1989; Nielsen et al. 1994) as indicated, unambiguously, by an Early Visean karstification of the Tournaisian to Lower Visean dolomites (Nielsen et al. 1994). Bedding parallel stylolites and fractures crosscut the dolomites. Karst cavities are filled by speleothem deposits (Nielsen et al. 1997) or by undolomitised crinoidal sediments, identical to the overlying limestones (Peeters et al. 1993). The dolomitisation is interpreted to result from the reflux of dense, saline brines (Dejonghe et al. 1989; Nielsen et al. 1994). These brines originated during formation of evaporites in the Givetian, Frasnian and Dinantian (Rouchy et al. 1986) and are the only possible source of the high-salinity fluids that were expelled in the Mesozoic. Part of them were also expelled in the Late Palaeozoic when they formed Frasnian synsedimentary barytes (Demaiffe and Dejonghe 1990; Heijlen et al. 2000). In order to explain the Ca and Na content of the fluids they must have been participating not only in the dolomitisation of the limestones, but also in a water–rock interaction that exchanged 2 $Na^+$ ions against 1 $Ca^{2+}$ ion in a systematic manner. Several authors consider albitisation of plagioclase as a likely reaction to accomplish this in sedimentary basins (Spencer 1987; Davisson et al. 1994; Davisson and Criss 1996). The Devonian and Lower Carboniferous rocks are poor in feldspars. Only the psammitic Fammennian rocks contain up to 45% of largely detrital K-feldspars (Michot 1963). Plagioclase is, however, abundant in the dacitic–rhyolitic rocks and the detrital arkoses of the Lower Palaeozoic basement (Vander Auwera and André 1985; André et al. 1986; Van Grootel et al. 1997). Therefore, the residual brines may have migrated into the basement where they interacted with siliciclastic rocks. Extensional faults, active during the Devonian and Early Carboniferous (Fielitz 1992, 1997), may have provided a path for the dense, saline fluids that were preserved in the deep subsurface during the Variscan deformation. Preservation of these fluids may relate to their migration into the subsurface to a depth that was little affected by Variscan thin-skinned tectonics. In the study area this would equate to a depth of at least 3 km (Hollman and Walter 1995). An additional argument for the migration of these high-salinity fluids to the subsurface is their recent recognition as fluid inclusions in ankerite veins in the Lower Devonian siliciclastics at the front zone in eastern Belgium (Muchez et al. 1998).

Large amounts of high-salinity fluids were found in the crystalline basement at depths of 4 km during the German Continental Deep Drilling Program (KTB; Möller et al. 1997). Behr et al. (1993) demonstrated and argued that high-salinity brines of Mesozoic origin are abundant at great depth (8–12 km) in western and central Europe. Because these fluids initially formed during the Permian, they remained in the subsurface for ~250 Ma. In contrast to this model, the high-salinity fluids in southern Belgium may originally have formed during the Palaeozoic, with migration of the mineralising brines to the place of ore deposition resulting from a suction pump mechanism during the Mesozoic extensional regime, as proposed by Redecke and Friedrich (1991) and Redecke (1992).

## Conclusions

Taking into account the anion geochemistry and geochemical evolution of the mineralising fluids and the sedimentary and tectonic setting, a palaeofluid flow model can be proposed for the high-salinity, Pb–Zn mineralising brines at the Variscan front zone. The high-density brines originally formed during the late Palaeozoic but, because of their high density, these fluids migrated into the subsurface, causing widespread early diagenetic dolomitisation. Their Ca and Na content, however, suggests that they migrated further downwards into the siliciclastic basement. Within this basement, the fluids probably interacted with plagioclase, causing albitisation that resulted in a further decrease of the Na content and an increase of the Ca content. During the Mesozoic, NNW-trending transverse extensional faults, related to the Rhine graben tectonism, intersected these basinal brines and allowed their upward migration, resulting in the deposition of lead and zinc ores in eastern Belgium.

**Acknowledgements** This research has been supported by the Fund for Scientific Research – Flanders (Belgium) grants G030097 N and G027499 N . We also would like to thank L. Dejonghe, R. Swennen and W. Viaene for stimulating discussions. H. Nijs kindly prepared the thin sections and the doubly polished wafers. The research of W. Heijlen is financed by the Flemish Institute for the Promotion of Scientific-Technological Research in the Industry (IWT). This research has been carried out within the GEODE programme of the European Science Foundation. Fluid inclusion studies at Leeds were in part funded by NERC grant GR3/11087. We are grateful to D. Kontak, an anonymous reviewer and the editor B. Lehmann for their constructive comments and suggestions on the manuscript.

## References


Anderson GM, Macqueen RW (1982) Ore deposit models-6. Mississippi Valley-type lead-zinc deposits. Geosci Can 9: 108–117

André L, Hertogen J, Deutsch S (1986) Ordovician–Silurian magmatic provinces in Belgium and the Caledonian orogeny in middle Europe. Geology 14: 879–882

Banks DA, Russell MJ (1992) Fluid mixing during ore deposition at the Tynagh base-metal deposit, Ireland. Eur J Mineral 4: 921–931

Banks DA, Yardley BWD (1992) Crush-leach analysis of fluid inclusions in small natural and synthetic samples. Geochim Cosmochim Acta 56: 245–248

Behr H-J, Gerler J (1987) Inclusions of sedimentary brines in post-Variscan mineralizations in the Federal Republic of Germany – a study by neutron activation analysis. Chem Geol 61: 65–77

Behr H-J, Horn EE, Frentzel-Beyme K, Reutel C (1987) Fluid inclusion characteristics of the Variscan and post-Variscan mineralizing fluids in the Federal Republic of Germany. Chem Geol 61: 273–285

Behr H-J, Gerler J, Hein UF, Reutel CJ (1993) Tectonic Brines und Basement Brines in den mitteleuropäischen Variszіden: Herkunft, metallogenetische Bedeutung und geologische Aktivität. Göttinger Arb Geol Paläont 58: 3–28

Bodine MW, Jones BF (1990) Normative analysis of groundwaters from the Rustler Formation associated with the Waste Isolation Pilot Plant (WIPP), southeastern New Mexico. Geochem Soc Spec Publ 2: 213–269

Bodnar RJ (1993) Revised equation and table for determining the freezing point depression of $H_2O$–NaCl solutions. Geochim Cosmochim Acta 57: 683–684

Bottrell SH, Yardley BWD, Buckley F (1988) A modified crush-leach method for the analysis of fluid inclusion electrolytes. Bull Mineral 111: 279–290

Carpenter AB (1978) Origin and chemical evolution of brines in sedimentary basins. Oklahoma Geol Surv Circ 79: 60–77

Carpenter AB, Trout ML, Pickett EE (1976) Preliminary report on the origin and chemical evolution of lead-and-zinc-rich oil field brines in central Mississippi. Econ Geol 69: 1191–1206

Cauet S, Weis D (1983) Lead isotope study of lead–zinc mineralization and its host sediments, Heure, Belgium: basis for a genetic model. Econ Geol 78: 1011–1016

Cauet S, Weis D, Herbosch A (1982) Genetic study of Belgian lead–zinc mineralisations in carbonate environments through lead isotopic geochemistry. Bur Rech Géol Min Bull II-4: 329–341

Charef A, Sheppard SMF (1988) The Malines Cambrian carbonate-shale-hosted Pb–Zn deposit, France: thermometric and isotopic (H, O) evidence for pulsating hydrothermal mineralization. Mineral Deposita 23: 86–95

Connolly CA, Walter LM, Baadsgaard H, Longstaffe FJ (1990) Origin and evolution of formation water, Alberta Basin, Western Canada Sedimentary Basin. 1. Chemistry. Appl Geochem 5: 375–395

Crocetti CA, Holland HD (1989) Sulfur–lead isotope systematics and the composition of fluid inclusions in galena from the Viburnum Trend, Missouri. Econ Geol 84: 2196–2216

Darimont A (1983) Inclusions fluides dans les calcites associées à la minéralisations Pb–Zn de Poppelsberg (Est de la belgique). Mineral Deposita 18: 379–386

Davisson ML, Criss RE (1996) Na–Ca–Cl relations in basinal fluids. Geochim Cosmochim Acta 60: 2743–2752

Davisson ML, Presser TS, Criss RE (1994) Geochemistry of tectonically expelled fluids from the northern Coast ranges, Rumsey Hills, California, USA. Geochim Cosmochim Acta 58: 1687–1699

Dejonghe L (1985) Contribution à l'étude métallogénique du synclinorium de Verviers (Belgique). Thèse de Doctorat d'Etat ès Sciences Naturelles, Université Pierre et Marie Curie, Paris

Dejonghe L (1986) Belgium. In: Dunning FW, Evans AM (eds) Mineral deposits of Europe, vol 3, Central Europe. Institution of Mining and Metallurgy and Mineralogical Society, London, p 99–102

Dejonghe L (1998) Zinc–lead deposits of Belgium. Ore Geol Rev 12: 329–354

Dejonghe L, Boulvain F (1993) Paleogeographic and diagenetic context of baritic mineralization enclosed within Frasnian perireefal formations: case history of the Chaudfontaine mineralization (Belgium). Ore Geol Rev 7: 413–431

Dejonghe L, Jans D (1983) Les gisements plombo-zincifères de l'Est de la Belgique. Chron Rech Min 470: 3–24

Dejonghe L, Guilhaumou N, Touray JC (1982) Les inclusions fluides de la barite du gisement sédimentaire de Chaudfontaine (provence de Liège, Belgique). Bull Soc Belge Géol 91: 79–89

Dejonghe L, Demaiffe D, Gorzawski H (1989) Géochimie isotopique (C, O, Sr) des dolomies frasniennes du Massif de Philippeville (synclinorium de Dinant, Belgique). Ann Soc Géol Belg 112: 87–102

de Magnée I (1967) Contribution à l'étude génétique des gisements belges de plomb, zinc et barytine. Econ Geol Monogr 3: 255–266

Demaiffe D, Dejonghe L (1990) Géochimie isotopique du strontium des barites, anhydrites, calcites et fluorites de Belgique. Ann Soc Géol Belg 113: 231–240

De Putter T, Rouchy JM, Herbosch A, Keppens E, Pierre C, Groessens E (1994) Sedimentology and paleo-environment of the Upper Visean anhydrite of the Franco-Belgian Carboniferous Basin (Saint-Ghislain borehole, southern Belgium). Sediment Geol 90: 77–93

Fielitz W (1992) Variscan transpressive inversion in the nortwestern Central Rhenohercynian belt of western Germany. J Struct Geol 14: 547–563

Fielitz W (1997) Inversion tectonics and diastathermal metamorphism in the Serpont massif area of the Variscan Ardenne (Belgium). Aardk Meded 8: 79–82

Fontes JC, Matray JM (1993) Geochemistry and origin of formation brines from the Paris Basin, France. 1. Brines associated with Triassic salts. Chem Geol 109: 140–175

Groessens E, Conil R, Hennebert M (1979) Le Dinantien du sondage de Saint-Ghislain. Mém Explor Cartes Géol Min Belg, vol 22

Hance L, Dejonghe L, Ghysel P, Laloux M, Mansy JL (1999) Influence of heterogeneous lithostructural layering on orogenic deformation in the Variscan Front Zone (eastern Belgium). Tectonophysics 309: 161–177

Heijlen W, Muchez P, Banks D, Nielsen P (2000) Origin and geochemical evolution of synsedimentary, syn- and posttectonic high salinity fluids at the Variscan thrust front in Belgium. J Geochem Expl 69–70: 149–152

Hollman G, Walter R (1995) The Variscan deformation front between Stavelot–Venn Anticline and Brabant Massif – a balanced geological cross section along the Liège–Theux traverse. N Jb Geol Paläont 2: 92–104

Kesler SE, Appold MS, Martini AM, Walter LM, Huston TJ, Kyle RJ (1995) Na–Cl–Br systematics of mineralizing brines in Mississippi Valley-type deposits. Geology 23: 641–644

Kesler SE, Martini AM, Appold MS, Walter LM, Huston TJ, Furman FC (1996) Na–Cl–Br systematics of fluid inclusions from Mississippi Valley-type deposits, Appalachian Basin: constrains on solute origin and migration paths. Geochim Cosmochim Acta 60: 225–233

Ladeuze F, Dejonghe L, Pauquet F (1991) Historique de l'exploitation des gisements plombo-zincifères de l'Est de la Belgique: le rôle de la 'Veille-Montagne'. Chron Rech Min 503: 37–50

Land LS, Prezbindowski DK (1981) The origin and evolution of saline formation water, Lower Cretaceous carbonates, south-central Texas, USA. J Hydrol 54: 51–74

Leach DL, Sangster DF (1993) Mississippi Valley-type lead zinc deposits. In: Kirkham RV, Sinclair WD, Thorpe RI, Duke JM

(eds) Mineral deposit modelling. Geol Assoc Can, Spec Pap 40: 289–314

McCaffrey MA, Lazar B, Holland HD (1987) The evaporation path of seawater and the coprecipitation of $Br^-$ and $K^+$ with halite. J Sediment Petrol 57: 928–937

Michot J (1963) Les feldspaths dans les sédiments dévoniens et carbonifères de la Belgique. Bull Ac R Belg, vol 34

Möller P, Weise SM, Althaus E, Bach W, Behr H-J, Borchardt R, Bräuer K, Drescher J, Erzinger J, Faber E, Hansen BT, Horn EE, Huenges E, Kämpf H, Kessels W, Kirsten T, Landwehr D, Lodeman M, Machon L, Pekdeger A, Pielow H-U, Reutel C, Simon K, Walther J, Weinlich FH, Zimmer M (1997) Paleofluids and Recent fluids in the upper continental crust: results from the German Continental Deep Drilling Program (KTB). J Geophys Res 102: 18233–18254

Muchez P, Sintubin M (1997) Palaeofluid flow evolution in a changing transpressive stress regime. In: Hendry J, Carey P, Parnell J, Ruffel A, Worden R (eds) Geofluids II. Anthony Rowe Ltd, Chippenham, pp 121–124

Muchez P, Sintubin M (1998) Contrasting origin of palaeofluids in a strike-slip fault system. Chem Geol 145: 105–114

Muchez P, Slobodnik M, Viaene W, Keppens E (1994) Mississippi Valley-type Pb–Zn mineralization in eastern Belgium: indications for gravity-driven flow. Geology 22: 1011–1014

Muchez P, Slobodnik M, Sintubin M, Viaene W, Keppens E (1997) Origin and migration of palaeofluids in the Lower Carboniferous of southern and eastern Belgium. Zentralbl Geol Paläont Teil I 11/12: 1107–1112

Muchez P, Zhang Y, Dejonghe L, Viaene W, Keppens E (1998) Evolution of palaeofluids at the Variscan thrust front in eastern Belgium. Geol Rundsch 87: 373–380

Nielsen P, Swennen R, Keppens E (1994) Multiple-step recrystallization within massive ancient dolomite units: an example from the Dinantian of Belgium. Sedimentology 41: 567–584

Nielsen P, Swennen R, Dickson JAD, Fallick AE, Keppens E (1997) Spheroidal dolomites in a Visean karst system – bacterial induced origin? Sedimentology 44: 177–195

Oakes CS, Bodnar RJ, Simonson JM (1990) The system NaCl–$CaCl_2$–$H_2O$: the ice liquidus at 1 atm total pressure. Geochim Cosmochim Acta 54: 603–610

Peeters C, Swennen R, Nielsen P, Muchez P (1993) Sedimentology and diagenesis of the Visean carbonates in the Vesdre area (Verviers Synclynorium, E-Belgium). Zentralbl Geol Paläont Teil 1 Heft 5: 519–547

Pelissonnier H (1967) Analyse paléohydrogéologique des gisements stratiformes de plomb, zinc, baryte, fluorite du type 'Mississippi Valley'. Econ Geol Monogr 3: 234–252

Redecke P (1992) Zur Geochemie und Genese variszischer und postvariszischer Buntmetallmineralisation in der Nordeifel und der Niederrheinischen Bucht. Mitt Mineral Lagerstättenkunde, vol 41

Redecke P, Friedrich G (1991) Constraints for sulfide mineralization in the Lower Rhine Basin, Germany. In: Pagel M, Leroy O (eds) Source, transport and deposition of metals. Balkema, Rotterdam, pp 481–484

Rouchy JM, Pierre C, Groessens E, Monty C, Laumondais A, Moine B (1986) Les évaporites pre-permiennes du segment varisque franco-belge: aspects paléogéographiques et structuraux. Bull Soc Belge Géol 95: 139–150

Samson I, Russell MJ (1987) Genesis of the Silvermines zinc–lead–barite deposit, Ireland: fluid inclusions and stable isotope evidence. Econ Geol 82: 371–394

Schneider J, Haack U, Hein UF, Germann A (1999) Direct Rb–Sr dating of sandstone-hosted sphalerites from stratabound Pb–Zn deposits in the northern Eifel, NW Rhenish Massif, Germany. In: Stanley et al. (eds) Mineral deposits: processes to processing. Balkema, Rotterdam, pp 1287–1290

Shepherd TJ, Rankin AH, Alderton DHM (1985) A practical guide to fluid inclusions studies. Chapman and Hall, New York

Spencer RJ (1987) Origin of Ca–Cl brines in Devonian formations, Western Canada Sedimentary Basin. Appl Geochem 2: 373–384

Vander Auwera J, André L (1985) Sur le milieu de depôt, l'origine des matériaux et le facies métamorphique de l'Assize de Tubize (Massif de Brabant, Belgique). Bull Soc Belge Géol 94: 171–184

Van Grootel G, Verniers J, Geerkens B, Laduron D, Verhearen M, Hertogen J, De Vos W (1997) Timing of magmatism, foreland basin development, metamorphism and inversion in the Anglo-Brabant fold belt. Geol Mag 134: 607–616

Viets JB, Leach DL (1990) Genetic implications of regional and temporal trends in ore fluid geochemistry of Mississippi Valley-type deposits in the Ozark region. Econ Geol 85: 842–861

Viets JB, Hofstra AH, Emsbo P (1996) Solute compositions of fluid inclusions in sphalerite from North American and European Mississippi Valley-type ore deposits: ore fluids derived from evaporated seawater. In: Sangster DF (ed) Carbonate-hosted lead–zinc deposits. Soc Econ Geol Spec Pub 4: 465–482

Weisbrod A, Poty B (1975) Thermodynamics and geochemistry of the hydrothermal evolution of the Mayres pegmatite (southeastern Massif Central, France). Pétrologie 1: 1–16

Wilkinson JJ, Jenkin GRT, Fallick AE, Foster RP (1995) Oxygen and hydrogen isotopic evolution of Variscan crustal fluids, south Cornwall, UK. Chem Geol 123: 239–254

Yardley BWD, Banks DA, Botrell SH (1993) Post-metamorphic gold–quartz veins from NW Italy: the composition and origin of the ore fluid. Miner Mag 57: 407–422